ELECTRON CLOUD MEASUREMENTS IN FERMILAB MAIN INJECTOR AND RECYCLER

J. Eldred, Department of Physics, Indiana University, Bloomington, IN 47405, USA
M. Backfish, C. Y. Tan, R. Zwaska, FNAL, Batavia, IL 60510, USA

Abstract

This conference paper presents a series of electron cloud measurements in the Fermilab Main Injector and Recycler. A new instability was observed in the Recycler in July 2014 that generates a fast transverse excitation in the first high intensity batch to be injected. Microwave measurements of electron cloud in the Recycler show a corresponding dependence on the batch injection pattern. These electron cloud measurements are compared to those made with a retarding field analyzer (RFA) installed in a field-free region of the Recycler in November. RFAs are also used in the Main Injector to evaluate the performance of beampipe coatings for the mitigation of electron cloud. Contamination from an unexpected vacuum leak revealed a potential vulnerability in the amorphous carbon beampipe coating. The diamond-like carbon coating, in contrast, reduced the electron cloud signal to 1% of that measured in uncoated stainless steel beampipe.

BACKGROUND

Electron cloud instabilities have been observed in a variety of modern proton accelerators [1–5]. Electron cloud was first observed in the Fermilab Main Injector in 2006 [6] and in the Fermilab Recycler in 2014 [7].

During the build-up of electron cloud, the particle beam causes the transverse acceleration of stray electrons which then scatter additional electrons from the beampipe. The number of electrons increase exponentially until a saturation is reached. The secondary electron yield (SEY) of a surface is the ratio of the average number of electrons scattered from the surface to the number of electron impacting the surface. The density of the electron cloud depends critically on beam intensity and SEY of the inner surface of the beampipe [8–10].

ELECTRON CLOUD MEASUREMENTS IN FERMILAB RECYCLER

Beginning in July 2014, a fast intensity-induced transverse instability was observed in the Recycler and limited operation until November. The instability has the unusual feature of selectively impacting the first high-intensity batch. A detailed description of the instability is given in [7]. The threshold of the instability is sensitive to batch intensity and bunch length, but recent studies in the Recycler demonstrated that the threshold of the instability was not sensitive to the azimuthal spacing of batches. Consequently, the prevailing theory is that the instability is caused by the electron cloud that is trapped [11, 12] in the gradient focusing dipoles of the Recycler [13]. In response to the instability, the electron cloud in the Recycler has been measured by retarding field analyzers (RFAs) and the dispersion of microwaves.

Microwave Measurements of the Recycler

The presence of electron cloud was measured in the Recycler by transmitting a microwave signal between a pair of two "split-plate" BPMs [14]. These studies follow the technique implemented in the Main Injector by Crisp et. al. in [15] and also by others elsewhere [16–18].

The first microwave measurement in the Recycler was conducted on August 20, 2014 by temporarily repurposing two Recycler BPMs (VP201 and VP203). During this measurement, the first batch was operating at an intensity of $\sim 3.6e12$ and subsequent batches at an intensity of $\sim 4.5e12$ per batch. During the pre-scheduled shutdown period from September 5 to October 23, spare Recycler BPMs (VP130 and VP202) were dedicated to the microwave experiment on a permanent basis. The second microwave measurement of the Recycler was conducted on December 18, 2014 using the new measurement location. At this time, the beampipe in the Recycler had conditioned and the instability no longer limited the operation of the Recycler. During the second measurement, the six batches each had an intensity of $\sim 4.4e12$.

A schematic of the electronic setup used for these studies is shown in Figure 1. The use of split-plate BPMs as improvised microwave antennas results in a ~ -80 dB transmission loss. Due to differences in the transmission spectrum at the two measurement locations [19], the second measurement was made at a carrier frequency of 2.060 GHz whereas the first measurement was made at 1.977 GHz.

The density of the electron cloud is modulated by the revolution harmonics of the proton beam (~90 KHz) and therefore the carrier frequency is phase-modulated (PM) in the presence of the electron cloud. Consequently, the electron cloud signal is seen as 90kHz sidebands on either side of the carrier frequency [7, 15]. The contribution that each batch makes to the sideband is $2\pi/7$ out of phase with the contribution made by the adjacent batch. This creates a possible ambiguity between changes in the density of the electron cloud and changes in the distribution of the electron cloud.

Figure 2 and Figure 3 show the first and second microwave measurement of the Recycler respectively. Each figure plots the average spectral power of the lower sideband frequency as a function of time within the Recycler cycle. The sharp feature in the beginning of each batch injection is composed of several sharp peaks, each declining in height with respect to the previous peak. The peaks are spaced at half-synchrotron period intervals and coincide with the minimums of the bunch length oscillation. The peaks in the

Copyright © 2015 CC-BY-3.0 and by the respective authors

Operated by Fermi Research Alliance, LLC under Contract No. De-AC02-07CH11359 with the United States Department of Energy.

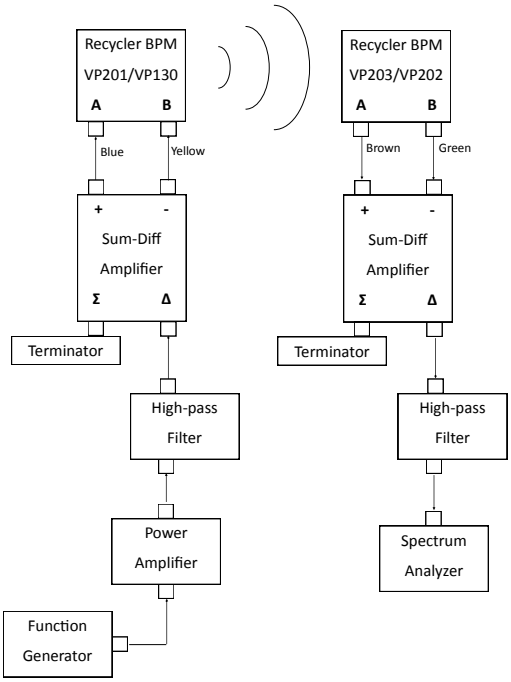

Figure 1: Flow-chart schematic of the microwave electron cloud measurement. The signal generator creates a signal at a single carrier frequency, next this signal propagates through the electron cloud, and lastly this signal is examined for phase modulation in the signal analyzer.

electron cloud measurement are a statistically significant margin above those in the beam background.

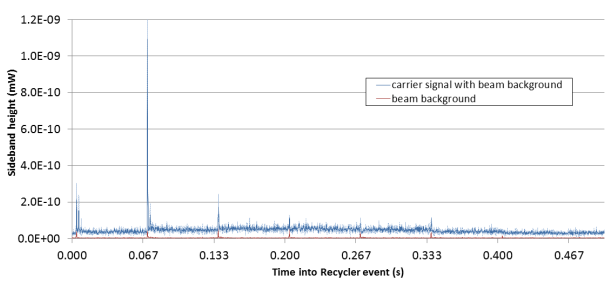

Figure 2: First microwave measurement. Spectral power of the lower sideband frequency averaged over 40 Recycler cycles and for each of two cases - with the carrier signal and without.

In the first measurement (Figure 2) the highest peaks in the electron cloud signal are obtained after the second batch injection, followed by the first, and then the others. Due to the batch structure used during the measurement [7], the magnitude of the horizontal oscillation induced by the instability followed the same pattern - greatest in the second batch, then the first, then the others. Similarly, the second measurement (Figure 3) peaks after the first batch injection which had the lowest instability threshold (due to the difference in batch structure).

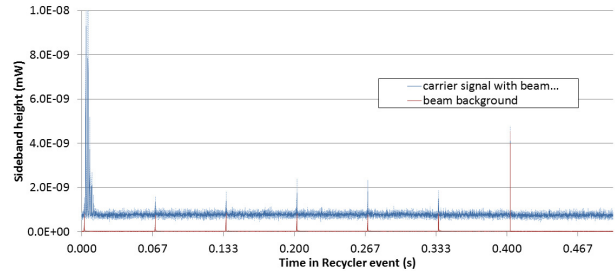

Figure 3: Second microwave measurement. Spectral power of the lower sideband frequency averaged over 40 Recycler cycles and for each of two cases - with the carrier signal and without.

RFA Measurements of the Recycler

During the pre-scheduled September-October shutdown an RFA electron cloud detector was installed in the Recycler at MI-52 [20] in a field-free region. Details about the design and characterization of the RFAs are given in [21] and [22].

Fig. 4 shows the RFA signal over the Recycler cycle on December 18, simultaneous with the microwave measurement shown in Fig. 3. Neither the pattern of the RFA nor the loss monitor [23] signal match the microwave measurements completely. However, the qualitative features – sharp peaks at injection declining in height and spaced at half-synchrotron intervals – are shared in the two measurements of the electron cloud. The discrepancy in the measurement likely stems from the fact that the microwave measurement detects electron cloud across an entire lattice cell whereas the RFA only measures a field-free region.

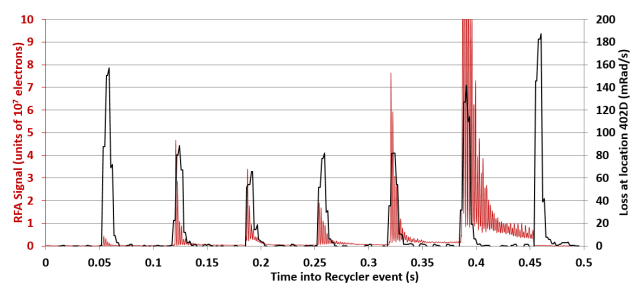

Figure 4: Signals from an RFA (red) measured in volts and a typical loss monitor (black) over the Recycler cycle.

MI-52 BEAMPIPE COATING TEST SITE

One promising way to reduce electron cloud formation is to coat the inside of the beampipe with low-SEY materials. The performance of beampipe coatings for mitigation of electron cloud have been tested in positron beams [24–26] and proton beams [27, 28]. Proposals have been made to apply an amorphous carbon (a-C) coating to the beampipe of CERN SPS by 2019, after commissioning Linac4 [29, 30].

In 2009, an experiment was installed at MI-52 of the Main Injector to measure the electron cloud in coated and uncoated beampipe. Figure 5 shows the measurement setup, with RFA1 residing in the uncoated section of beampipe,

Copyright © 2015 CC-BY-3.0 and by the respective authors

ISBN 978-3-95450-168-7

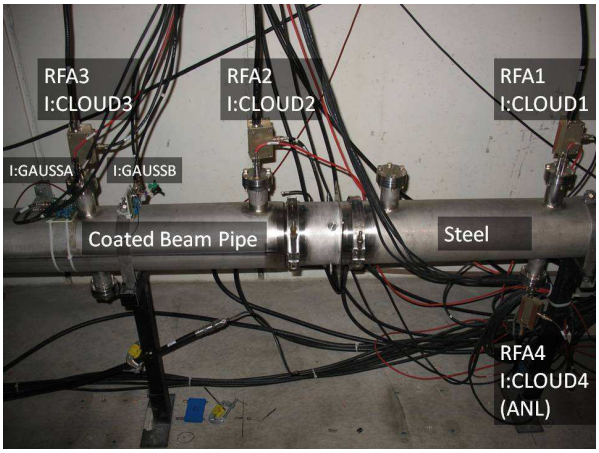

Figure 5: The electron cloud measurement setup in the Main Injector at MI-52. The setup primarily consists of four RFAs and two beampipe sections. The beampipe is 6" in diameter and the coated and uncoated sections are each ~1 meter long. The setup is located in a straight section to avoid electron confinement from magnets.

RFA2 residing just inside the coated section of beampipe, and RFA3 residing in the center of the coated section of beampipe. The MI-52 test site was used to measure the performance of titanium nitride (TiN) and a-C beampipe coatings in 2009 and 2010 [22]. Yin Vallgren's dissertation [31] provides a detailed description of preparation and aging studies of a-C coated beampipe.

In [22], we analyzed the electron cloud at each location by forming a daily scatterplot of the electron cloud signal as a function of beam intensity and fitting it with an exponential function. From the exponential fit we derive a benchmark beam intensity x_0, the beam intensity at which the electron cloud flux is 10^7 electrons per cm^2 per second.

In particular, one result from the a-C test in [22] merits further discussion. Figure 6 tracks the benchmark x_0 over time to compare the performance and conditioning of the beampipe at each location. On August 31, 2010, an early vacuum leak near the downstream (RFA3) end of the installation resulted in a dramatic change in the apparent conditioning of the a-C beampipe. The benchmark recorded at RFA3 decreases suddenly and lags relative to the benchmark recorded 41 cm upstream at the RFA2 location. At periods of the low beam intensity, the a-C beampipe at RFA3 seems to decondition more rapidly than the beampipe at the other two locations. For most of the run, the a-C coated beampipe exposed to the vacuum leak (RFA3) performs worse than or comparable to the uncoated beampipe (RFA1), whereas the a-C coated beampipe farther from the vacuum leak (RFA2) performs consistently better.

In 2013, a diamond-like carbon (DLC) beampipe was prepared for us by KEK [24] and a test of this material was initiated. This test does not yet contain any beam intensity data above 28×10^{12} protons because the run period coincided with the commissioning of the Recycler [32]. Consequently

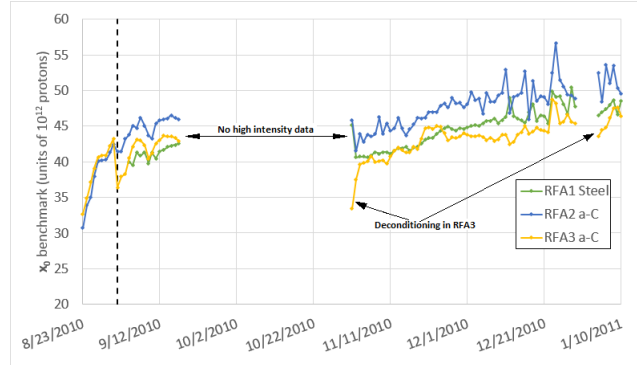

Figure 6: The daily fit of the x_0 benchmark is shown over time for RFA1 (steel), RFA2 (a-C near steel), and RFA3 (a-C). After a vacuum leak occurs (dashed line) near to RFA3, the x_0 benchmark for RFA3 decreases dramatically and lags behind RFA2.

no conditioning was observed after the first two weeks in any sample. The intensity benchmark x_0 stayed below 30×10^{12} and was dependent on beam quality (bunch length, spot size, and vacuum conditions). We will continue this experiment for another year in order to track the conditioning behavior of the DLC.

In the DLC data we have to date, the RFA2 signal is 10% to 15% of the RFA1 signal and the RFA3 is 0.5% to 1% of the RFA1 signal. The RFA2 signal is primarily seeded by electrons propagated from the denser electron cloud in the stainless steel beampipe 5 cm away. The contribution that seeding from the stainless steel makes to the RFA3 signal is not known.

CONCLUSION

The Recycler measurements have a direct relevance to intensity upgrades at Fermilab and also underscore the potential diversity of electron cloud phenomena. The measurements of the electron cloud in the Recycler show unusual sensitivity to batch structure and bunch-length that mirror the features of a correspondingly unusual instability in the Recycler. The microwave measurements have served effectively as a rapid diagnostic technique that can be implemented with pre-existing accelerator hardware.

Main Injector measurements of electron cloud provide an important counterpoint to previous accelerator tests of beampipe coatings for electron cloud mitigation. A fortuitous vacuum leak at the test location suggests that the robustness of the a-C coating could be a major concern. In contrast, preliminary results on the DLC coating are very promising – a factor of 100-200 decrease in electron cloud flux at a given beam intensity.

ACKNOWLEDGMENTS

This work is supported in part by grants from the US Department of Energy under contract DE-FG02-12ER41800 and the National Science Foundation NSF PHY-1205431.

Copyright © 2015 CC-BY-3.0 and by the respective authors

REFERENCES

[1] G. Arduini, T. Bohl, K. Cornelis et al., Proc. ECLOUD04, [http://mafurman.lbl.gov/ECLOUD04_proceedings/arduini-ga_ecloud04_v2.pdf].

[2] G. Iadarola, H. Bartosik, G. Rumolo et al., Proc. IPAC14, [www.jacow.org/IPAC2014/papers/tupme027.pdf].

[3] W. Fischer, M. Blaskiewicz, J. M. Brennan et al., Phys. Rev. Lett. **11**, 041002 (2008) [http://journals.aps.org/prstab/pdf/10.1103/PhysRevSTAB.11.041002].

[4] R. J. Macek, A. Browman, D. Fitzgerald et al., Proc. PAC01, [http://accelconf.web.cern.ch/AccelConf/p01/PAPERS/FOAB007.PDF].

[5] M. Blaskiewicz, M. A. Furman, M. Pivi et al., Phys. Rev. Lett. **6**, 014203 (2003) [http://journals.aps.org/prstab/pdf/10.1103/PhysRevSTAB.6.014203].

[6] X. Zhang, A. Z. Chen, W. Chou et al., Proc. PAC07, [http://accelconf.web.cern.ch/AccelConf/p07/PAPERS/THPAN117.PDF].

[7] J. Eldred, P. Adamson, D. Capista et al., Proc. HB2014, [www.jacow.org/HB2014/papers/tho4lr04.pdf].

[8] R. M. Zwaska, Proc. PAC11, [http://accelconf.web.cern.ch/AccelConf/PAC2011/papers/MOOBS4.PDF].

[9] P. L. G. Lebrun. P. Spentzouris, J. R. Cary et al., Proc. ECLOUD10, [www.jacow.org/ECLOUD2010/papers/MOD03.pdf].

[10] M. A. Furman, LBNL Report No. LBNL-4215E/CBP Note 868, 2011, [http://mafurman.lbl.gov/LBNL-4215E.pdf].

[11] P. J. Channell, JINST **4**, P08008 (2009) [http://iopscience.iop.org/1748-0221/4/08/P08008/pdf/1748-0221_4_08_P08008.pdf].

[12] R, J. Macek, A. A. Browman, J. E. Ledford et al., Phys. Rev. Lett. **11**, 010101 (2008) [http://journals.aps.org/prstab/pdf/10.1103/PhysRevSTAB.11.010101].

[13] P. Karns, C. Gattuso, M. Hue et al., Recycler Rookie Book, 2013 [http://www-bdnew.fnal.gov/operations/rookie_books/Recycler_RB_v1.42.pdf].

[14] J. Fitzgerald, J. Crisp, E. McCrory et al., AIP Conf. Proc. **451**, 370 (1998) [http://scitation.aip.org/content/aip/proceeding/aipcp/10.1063/1.57018].

[15] J. Crisp, N. Eddy, I. Kourbanis et al., Proc. PAC09, [www.jacow.org/d09/papers/tupb23.pdf].

[16] S. De Santis, J. M. Byrd, F. Caspers et al., Phys. Rev. Lett. **100**, 094801 (2008) [http://journals.aps.org/prl/pdf/10.1103/PhysRevLett.100.094801].

[17] S. Federmann, F. Caspers, E. Mahner, Phys. Rev. ST Accel. Beams **14**, 012802 (2011) [http://journals.aps.org/prstab/pdf/10.1103/PhysRevSTAB.14.012802].

[18] S. De Santis, J. Sikora, D. Alesini et al., Proc. IPAC12, [www.jacow.org/IPAC2012/papers/MOPPR073.PDF].

[19] J. Eldred, Fermilab Report No. Beams-doc-4760-v1, 2015, [https://beamdocs.fnal.gov/AD-private/DocDB/ShowDocument?docid=4760].

[20] T. Asher and S. Baginski, Main Injector Rookie Book, 2013 [http://www-bdnew.fnal.gov/operations/rookie_books/Main_Injector_v1.1.pdf].

[21] C. Y. Tan, K. L. Duel, R. Zwaska, Proc. PAC09, [http://accelconf.web.cern.ch/AccelConf/pac2009/papers/th5rfp041.pdff].

[22] M. Backfish, Masters thesis, Indiana University, 2013 [http://inspirehep.net/record/1294079/files/fermilab-masters-2013-03.pdf].

[23] A. Baumbaugh, C. Briegel, B. C. Brown et al., JINST **6**, T11006 (2011) [http://iopscience.iop.org/1748-0221/6/11/T11006/pdf/1748-0221_6_11_T11006.pdf].

[24] M. Nishiwaki and S. Kato, Proc. IPAC10, [http://accelconf.web.cern.ch/AccelConf/IPAC10/papers/thpea079.pdf]

[25] J. R. Calvey, W. Hartung, Y. Li et al., Nucl. Instrum. Meth. A **760**, 86 (2014) [http://www.sciencedirect.com/science/article/pii/S0168900214005786].

[26] M. T. F. Pivi, J. S. T. Ng, D. Arnett et al., Proc. EPAC08, [http://accelconf.web.cern.ch/AccelConf/e08/papers/mopp063.pdf].

[27] C. Yin Vallgren, G. Arduini, J. Bauche et al., Phys. Rev. Lett. **14**, 071001 (2011) [http://journals.aps.org/prstab/pdf/10.1103/PhysRevSTAB.14.071001].

[28] C. Yin Vallgren, P. Chiggiato, P. Costa Pinto et al., Proc. IPAC11, [http://accelconf.web.cern.ch/AccelConf/IPAC2011/papers/TUPS028.PDF].

[29] S. S. Gilardoni, G. Arduini, T. Argyropoulos et al., Proc. HB2012, [https://accelconf.web.cern.ch/accelconf/HB2012/papers/tuo1a01.pdf].

[30] P. Costa Pinto, A. Bellunato, T. Basso et al., Proc. IPAC14, [http://accelconf.web.cern.ch/accelconf/IPAC2014/papers/wepri043.pdf].

[31] C. Yin Vallgren, Doctoral dissertation, Chalmers University Of Technolog, 2011 [http://cds.cern.ch/record/1374938/files/CERN-THESIS-2011-063.pdf?version=2].

[32] I. Kourbanis, RR Slip Stacking and Beam Power, presented at March 16 2015 Fermilab All Experimenter's Meeting [https://fnal.gov/directorate/program_planning/all_experimenters_meetings/special_reports/Kourbanis_RR%20slip%20stacking%20and%20Beam%20Power_AEM_3172015.pdf].

Copyright © 2015 CC-BY-3.0 and by the respective authors

ISBN 978-3-95450-168-7